



HAL
open science

Adaptive trade-offs between vertebrate defence and insect predation drive Amazonian ant venom evolution

Axel Touchard, Samuel D Robinson, Hadrien Lalagüe, Steven Ascoët, Arnaud Billet, Alain Dejean, Nathan J Téné, Frédéric Petitclerc, Valérie Troispoux, Michel Treilhou, et al.

► To cite this version:

Axel Touchard, Samuel D Robinson, Hadrien Lalagüe, Steven Ascoët, Arnaud Billet, et al.. Adaptive trade-offs between vertebrate defence and insect predation drive Amazonian ant venom evolution. Proceedings of the Royal Society B: Biological Sciences, 2024, 291 (2035), 10.1098/rspb.2024.2184 . hal-04795576

HAL Id: hal-04795576

<https://hal.science/hal-04795576v1>

Submitted on 21 Nov 2024

HAL is a multi-disciplinary open access archive for the deposit and dissemination of scientific research documents, whether they are published or not. The documents may come from teaching and research institutions in France or abroad, or from public or private research centers.

L'archive ouverte pluridisciplinaire **HAL**, est destinée au dépôt et à la diffusion de documents scientifiques de niveau recherche, publiés ou non, émanant des établissements d'enseignement et de recherche français ou étrangers, des laboratoires publics ou privés.



Distributed under a Creative Commons CC0 - Public Domain Dedication 4.0 International License

1 **Main Manuscript for**

2 **Adaptive trade-offs between vertebrate defense and insect**
3 **predation drive Amazonian ant venom evolution**

4 Axel Touchard^{1,2,†} Samuel D. Robinson³, Hadrien Lalagüe¹, Steven Ascoët⁴, Arnaud Billet⁴, Alain
5 Dejean^{1,5}, Nathan J. Téné⁴, Frédéric Petitclerc¹, Valérie Troispoux⁶, Michel Treilhou⁴, Elsa
6 Bonnafé⁴, Irina Vetter^{3,7}, Joel Vizúeta⁸, Corrie S. Moreau², Jérôme Orivel^{1,*}, Niklas Tysklind^{6,*}

7 ¹CNRS, UMR Ecologie des forêts de Guyane – EcoFoG (AgroParisTech, CIRAD, INRAE,
8 Université de Guyane, Université des Antilles), Campus Agronomique, BP 316, 97379 Kourou
9 Cedex, France.

10 ²Department of Entomology, Cornell University, Ithaca, New York, USA.

11 ³Institute for Molecular Bioscience, The University of Queensland, QLD 4072, Australia.

12 ⁴Equipe BTSB-EA 7417, Université de Toulouse, Institut national universitaire Jean-François
13 Champollion, Place de Verdun, 81012, Albi, France.

14 ⁵Centre de Recherche sur la Biodiversité et l'Environnement, Université de Toulouse, CNRS,
15 Toulouse INP, Université Toulouse 3 – Paul Sabatier (UPS), Toulouse, France.

16 ⁶INRAE, UMR Ecologie des forêts de Guyane - EcoFoG (AgroParisTech, CIRAD, CNRS,
17 Université de Guyane, Université des Antilles), Campus Agronomique, BP 316, 97379 Kourou
18 Cedex, France.

19 ⁷School of Pharmacy, The University of Queensland, Woolloongabba, QLD 4102, Australia.

20 ⁸Villum Centre for Biodiversity Genomics, Section for Ecology and Evolution, Department of
21 Biology, University of Copenhagen, Copenhagen, Denmark.

22 *These authors contributed equally to this work.

23 †Axel Touchard (A.T.)

24 **Email:** axel.touchard2@gmail.com (A.T.)

25 **Author Contributions:** A.T., J.O., and N.T. designed research; A.T., S.D.R., H.L., S.A., N.J.T.,
26 V.T., F.P., and A.B. performed research; J.O., N.T., E.B., M.T., I.V., and C.S.M. contributed
27 resources; A.T., S.D.R., and H.L. analyzed data; A.T. wrote the manuscript; all authors have read
28 and agreed to the published version of the manuscript.

29 **Competing Interest Statement:** Authors declare no competing interests.

30 **Acknowledgments**

31 We thank Wolfgang Wüster and Nicholas Casewell for valuable input into the experimental
32 design. We thank Philippe Gaucher for providing a colony of *Pseudomyrmex viduus*. We thank
33 Federica Catonaro, Elena di Barbora, and Emanuela Aleo for assistance with transcriptome
34 library construction and sequencing. Ant samples were collected under the authorizations of the
35 French Ministry of Ecological and Solidarity Transition, in accordance with Article 17, paragraph
36 2, of the Nagoya Protocol on Access and Benefit-sharing (Reference number of the permit:
37 TREL1916196S/214).

38

39 **Fundings**

40 This research was funded by Investissement d'Avenir grant of the Agence Nationale de la
41 Recherche (CEBA: ANR- 10-LABX-25-01) and by the PO-FEDER 2014–2020, Région Guyane
42 (FORMIC, GY0013708).

43 **Keywords:** Hymenoptera; Formicidae; Sting; Neurotoxin; Cytotoxic peptide; Defensive traits

44 **This PDF file includes:**

45 Main Text
46 Figures 1 to 3
47

48 **Abstract**

49 Stinging ants have diversified into various ecological niches, and selective pressures may
50 have contributed to shape the composition of their venom. To explore the drivers underlying
51 venom variation in ants, we sampled 15 South American rainforest species and recorded a range
52 of traits, including ecology, morphology, and venom bioactivities. Principal component analysis of
53 both morphological and venom bioactivity traits reveal that stinging ants display two functional
54 strategies where species have evolved toward either an exclusively offensive venom or a
55 multifunctional venom. Additionally, phylogenetic comparative analysis indicates that venom
56 function (predatory, defensive, or both) and mandible morphology correlate with venom bioactivity
57 and volume. Further analysis of the venom biochemistry of the 15 species revealed switches
58 between cytotoxic and neurotoxic venom compositions among species. Our study supports an
59 evolutionary trade-off between the ability of venom to deter vertebrate predators and to paralyze
60 insect prey which are correlated with different venom compositions and life history strategies
61 among Formicidae.

62 **1. Introduction**

63 Most ants have venom, the composition of which can vary considerably among lineages; some
64 species have formic acid or alkaloid-based venoms, while the venoms of most stinging species
65 are peptidic [1]. Among different lineages of stinging ants, venoms can exhibit very different
66 peptide toxin profiles [2,3], presumably in response to distinct functional uses. The Formicidae
67 have radiated into diverse ecological niches [4], and numerous evolutionary forces may have
68 contributed to the shaping of their venoms. Here, we evaluate several ecological factors that can
69 be considered as potential drivers of venom evolution in ants:

70 (i) Foraging activities of predatory ants range from subterranean to canopy habitats. We
71 hypothesized that predatory venom efficacy is more important for arboreal ants that need to
72 subdue prey rapidly to prevent it from falling to the ground, leading to highly paralytic venom.
73 Previous research on ponerine ants suggested that arboreal habits may influence the efficacy of
74 venom in capturing prey [5].

75 (ii) Diet is often a potent driver of venom evolution in predatory organisms [6]. Many predatory
76 ants use their venom to capture a diversity of prey; however, several species or lineages are
77 stenophagous (i.e. prey exclusively on a restricted group of arthropods) [7]. Venoms of
78 stenophagous ants may therefore be more effective on their intended prey, while greater
79 taxonomic diversity of prey would lead to more complex venom compositions [8–10].

80 (iii) As most stinging ants also use their mandibles to subdue their prey before delivering the
81 paralyzing sting, mandible shape varies widely, which could be linked to venom composition. The

82 morphology of the mandibles of some predatory ants is indeed specialized to the shape of the
83 prey [7,11], while trap-jaw ants use spring-loaded mandibles that snap shut on prey with high
84 speed and force [12]. The presence of specialized trap-jaw mandibles, which enable efficient
85 physical capture of prey, might be negatively correlated with venom amount and efficacy to
86 paralyze insect prey as an ecological trade-off.

87 (iv) Ants that live in mutualistic association with myrmecophytes (e.g. acacia ants) use their
88 venom not for predation, but for fierce protection of the host plant [13], while in contrast, some
89 stinging species lack aggression toward potential predators [14]. These non-aggressive ants
90 exhibit thanatosis (i.e. feigning death) [15], escape behavior [16], or rely on morphological
91 attributes such as spines as a deterrent rather than using their sting against vertebrate predators
92 [17]. Venom function, whether predatory, defensive, or both, is therefore a putative driver of
93 venom composition in ants. We hypothesize that selective pressures for defense have led ants to
94 produce large amounts of venom comprising painful toxins, while ants that primarily use their
95 venom to subdue prey would deliver a small amount of highly effective venom to paralyze insects.

96 We designed a phylogenetically nested sampling of South American rainforest ant
97 genera, each with several congeneric species with contrasting ecological traits. The genera were
98 selected at different phylogenetic distances: sister genera, genera within the same subfamily, and
99 genera from different families, to evaluate if the obtained signals were conserved across the
100 phylogeny. Our sampling was mainly based on foraging activity: arboreal vs terrestrial. The effect
101 of foraging activity on venom was tested in three genera of the subfamily of Ponerinae (i.e.
102 *Anochetus*, *Odontomachus*, and *Neoponera*) and in a fourth non-ponerine genus,
103 *Pseudomyrmex*. Ponerinae are a basal lineage of ants while Pseudomyrmecinae represent a
104 more derived subfamily. We also extended our sampling to two other arboreal ant species
105 (*Daceton armigerum* and *Paraponera clavata*), since previous studies had highlighted unusual
106 venom compositions [2,18]. This sampling also gave us the opportunity to gain insight into how
107 other potential ecological factors may contribute to the shaping of ant venom. Two species were
108 presumed to be stenophagous: *Neoponera commutata* is a known specialized termite predator
109 [19] and *Anochetus emarginatus* is also suspected to be a termite specialist [20,21] in contrast
110 with their respective congeners included here. The inclusion of *D. armigerum* allowed testing the
111 convergent effects of trap-jaw mandibles on venom evolution with the sister genera
112 *Odontomachus* and *Anochetus* [12]. *Paraponera clavata*, known as the bullet ant and notable for
113 its painful defensive sting [22], was also included in this panel as a venom that has evolved to
114 effectively repel vertebrate predators. Within the genus *Pseudomyrmex*, we used ground-dwelling
115 (*P. termitarius*) and arboreal (*P. gracilis*) predatory species and compared them with obligate
116 plant-ant species (*P. viduus* and *P. penetrator*), which never use their venoms for predation [23],
117 to examine the effects of relaxed selection pressures for predatory capacity on venom diversity.

118 To date, no studies have integrated ecological traits, biochemical composition, and
119 bioactivities in a phylogenetic framework to explore the factors that lead to distinct venom
120 compositions in ants and, more broadly, very few in other venomous lineages [24]. To evaluate
121 the impact of the abovementioned ecological traits on ant venoms we analyzed stinging behavior,
122 diet, a suite of morphological traits, venom activities, and venom composition while controlling for
123 phylogenetic relationships. Among morphological traits we measured length of the sting and
124 mandibles since ants use both to capture prey and to defend against predators leading to the
125 hypothesis that a long sting would be associated with a defensive function, while long mandibles
126 would allow for better seizure of prey. We evaluated the volume of the whole venom reservoir to
127 provide information on the metabolic cost of venom production. Venom activities on blowflies and
128 mouse sensory neuronal cells informed on venom efficacy to subdue insects and deter

129 vertebrates. To provide insights into the mechanism of action of the venoms, we evaluated their
130 cytotoxicity against *Drosophila* cells using two assays that measure the effect on cell metabolism
131 and membrane cell integrity. Finally, to understand the biochemical mechanisms underlying the
132 observed variations in venom activities and modes of action, we examined the venom
133 composition of each of the 15 species and discussed the results in light of the life history of each
134 ant species.

135 **2. Material and Methods**

136 **(a) Ants and venom samples preparation**

137 Live specimens of worker ants from different colonies for each species were collected in French
138 Guiana. Two additional ant species were originally included in the sampling design (*A. targionii*
139 and *P. tenuis*) but could not be investigated because of the low amount of venom obtained. To
140 identify transcripts involved in venom production, we aimed to generate whole-body (i.e. head
141 and thorax) and venom gland transcriptomes for each species, and then, subtract transcripts
142 expressed in the whole-body transcriptome from those in the venom gland, to identify those
143 transcripts expressed largely in venom glands. For each species we dissected: 1) both venom
144 glands and venom reservoirs from 100 live workers per species in ultrapure water and
145 immediately placed in 1 mL of RNeasy Lysis Buffer (Thermo Fisher Scientific, Waltham, MA, USA); and 2)
146 the head and thorax of 2-3 workers in 1 mL of RNeasy Lysis Buffer. Samples were stored at -80°C prior to
147 RNA extraction. Crude venom samples were prepared by dissecting ant venom reservoirs in
148 ultrapure water, then pooled in 10% acetonitrile (ACN) in ultrapure water and stored at -20°C
149 prior to freeze-drying. Venom samples were then loaded onto a 0.45 μm Costar[®] Spin-X tube
150 filter (Corning Incorporated, Corning, NY, USA) and centrifuged at 12,000 g for 3 min to remove
151 tissues from the venom apparatus. Filtered venom samples were then lyophilized, weighed, and
152 stored at -20°C until further use. For each species we also estimated the venom yield, i.e. the
153 weight of freeze-dried venom from a pool of several individual venom reservoirs divided by the
154 number of dissected workers. This value provides an estimate of the maximum amount of venom
155 that an individual worker would be capable of delivering.

156 **(b) Venom composition and transcripts classification**

157 To characterize the venom composition of each species we employed a transcriptomic approach
158 coupled with mass spectrometry to validate the presence of peptides in the venom (the proteo-
159 transcriptomic method is described in electronic supplementary material, supporting methods).
160 From the transcriptomes generated, the annotations were manually curated focusing on
161 transcripts coding for toxins, with consideration of gene expression levels in venom glands and in
162 the body. We also selected and examined additional transcripts based on precursor similarities to
163 known toxin peptides. A total of 465 transcripts encoding putative toxins were retained for
164 subsequent analyses (electronic supplementary material, Figure S1 and Dataset S1). Proteomic
165 data were generated from the mass spectrometry fragmentation spectra using PEAKS software
166 [25], with the transcriptome of each species implemented as a database for peptide sequence
167 assignment. Positive matches of proteomics data with transcripts allowed us to confirm 305
168 peptide sequences. Total ion chromatograms were also generated with crude venoms and the
169 LC-MS profile annotated (electronic supplementary material, Figure S2-3). Peptide transcripts
170 were clustered into five gene clades (i.e. cysteine-rich poneritoxin, ponericin-like,
171 pseudomyrmecitoxin (PSDTX), ICK-PONTX, dimeric myrmecitoxin (MYRTX)) according to the
172 predictive signal sequence (electronic supplementary material, Figure S4). To define gene
173 clades, we used an approach based on similarity of signal parts. Signal parts were predicted

174 using SignalP - 6.0 server [26] and then aligned using the Muscle program in MEGA-X [27]. A
175 pairwise distance matrix between sequences was extracted from the multiple alignments and
176 used for HCA clustering using the hclust function with the ward method from the R package
177 "stats". Transcripts were further manually classified into families based on the similarity of the
178 amino acid sequences of the whole precursors (signal, pro-, and mature regions). For each
179 family, multiple alignments of full-length precursors were generated using the Muscle program in
180 MEGA-X version 10.1.8 [27] and edited using Jalview version 2.11.2.7 [27,28]. We classified the
181 transcripts into 62 peptide families and 3 enzyme toxins (i.e. phospholipase A₁, phospholipase A₂,
182 and venom allergen 3) (electronic supplementary material, Figure S5-12). The full list of
183 transcripts expressed in venom glands with a TMM greater than 100, the identified toxin
184 precursor sequence, the predicted mature part, the family assignment, and PEAKS results can be
185 found in Dataset S1. The venom composition of *Pa. clavata*, previously published by Aili *et al* [18]
186 has been included in our analysis. A total of 14 toxin families (i.e. families 23, 26, 29, 33, 34, 35,
187 37, 49, 52, 54, 56, and 59) were not included in the venom composition analysis for clustering
188 because no transcript sequences could be confirmed by mass spectrometry, yet they were
189 retained in the sequence alignments. For venom clustering, a Bray-Curtis distance matrix based
190 on the relative expression of the toxin family was generated using the veggdist function from the
191 R package "vegan" [29], followed by hierarchical clustering analysis (HCA) using the hclust
192 function with the full method from the R package "stats" [30]. The dendlist function from the R
193 package "dendextend" [31] was used to plot and align the species phylogeny tree with the venom
194 composition HCA cladogram. The final Figure 2 was edited in GraphPad Prism v10.0.3.

195 **(c) Morphological traits**

196 Six morphological traits were measured on up to 13 randomly selected workers per species.
197 Measurements were made using an ocular micrometer accurate to 0.01 mm mounted on a Leica
198 M80 or Leica S9E stereomicroscope (Leica Microsystems, Heerbrugg, Switzerland). The traits
199 considered were Weber's length (i.e., the diagonal length of the mesosoma in profile view, which
200 is a proxy for worker size [32], head length, mandible length, sting length, venom reservoir length,
201 and venom reservoir width. We estimated the venom reservoir volume using the standard
202 ellipsoid formula; $\pi/6$ (venom reservoir length \times venom reservoir width²). For analysis we used
203 size/volume-corrected ratios calculated as follows: mandible proportion (mandible length / head
204 length), sting proportion (sting length / Weber's length), venom reservoir proportion (venom
205 reservoir volume / Weber's length³).

206 **(d) Neuronal cell assays**

207 As a proxy for pain in vertebrates, we assessed the potency of each of the 15 venoms to activate
208 mammalian neuronal cells, defined as an increase in intracellular Ca²⁺ concentration ([Ca²⁺]_i) in
209 the F11 (mouse neuroblastoma \times rat dorsal root ganglion (DRG) neuron hybrid) cell line. F11
210 were maintained on Ham's F12 media supplemented with 10% FBS, 100 μ M hypoxanthine, 0.4
211 μ M aminopterin, and 16 μ M thymidine (Hybri-Max, Sigma Aldrich). 384-well imaging plates
212 (Corning, Lowell, MA, USA) were seeded 24 h prior to calcium imaging, resulting in ~90%
213 confluence at the time of imaging. Cells were loaded for 30 min at 37°C with Calcium 4 assay
214 component A in physiological salt solution (PSS; 140 mM NaCl, 11.5 mM D-glucose, 5.9 mM KCl,
215 1.4 mM MgCl₂, 1.2 mM NaH₂PO₄, 5 mM NaHCO₃, 1.8 mM CaCl₂, 10 mM HEPES) according to
216 the manufacturer's instructions (Molecular Devices, Sunnyvale, CA). Ca²⁺ responses were
217 measured using a FLIPRPenta fluorescent plate reader equipped with a CCD camera (Ex: 470 to

218 490 nm, Em: 515 to 575 nM) (Molecular Devices, Sunnyvale, CA). Signals were read every
219 second for 10 s before, and 300 s after, the addition of venoms (in PSS supplemented with 0.1%
220 BSA). The pain-causing capacity of a given species' venom is a product of both the venom
221 potency and amount of venom able to be delivered. By dividing the average venom yield (μg) by
222 venom potency ($\mu\text{g}/\text{mL}$) we calculated a value we refer to as the nocifensive capacity for each
223 species.

224 **(e) Insect activity assays**

225 To assess the potency of venoms to paralyze and to kill invertebrate prey, we injected different
226 doses of crude venom into the blowfly *Lucilia caesar* (the average mass of flies was 19 ± 2 mg).
227 Blowfly larvae (*Lucilia caesar*) were purchased from a fisheries shop (Euroloisir81, Lescure-
228 d'Albigeois, France) and kept at 25°C until hatching. Flies 1-4 days after hatching were used for
229 injection assays. Blowfly assays were done through lateral intrathoracic injection of $1 \mu\text{L}$ of
230 venom dissolved in ultra-pure water at various concentrations using a fixed 25-gauge needle
231 attached to an Arnold hand microapplicator (Burkard Manufacturing Co., Ltd., Rickmansworth,
232 UK) with a 1.0 mL Hamilton Syringe (1000 Series Gastight, Hamilton Company, Reno, NV, USA).
233 Then, the blowfly was placed in an individual 2 mL tube containing $15 \mu\text{L}$ of 5% glucose solution.
234 Paralysis was monitored at 1 h and 24 h post-injection, while lethality was monitored at 24 h.
235 Flies that did not display any signs of movement dysfunction were considered unaffected,
236 otherwise they were recorded as paralyzed. Flies were deemed dead if they did not respond at all
237 to tweezer mechanical stimulation when observed under a dissecting microscope. Ten flies were
238 used for each toxicity experiment and for the corresponding control (ultrapure water solution).
239 Each dose was repeated three times. Dose–response data were analyzed to determine a half
240 maximal paralytic dose (PD_{50}) and a half maximal lethal dose (LD_{50}). The paralytic and lethal
241 capacities of the species were calculated as for the nocifensive capacity (see section neuronal
242 cell assays).

243 **(f) Cytotoxicity and membrane potential assays**

244 *Drosophila* S2 cells (Thermofisher, USA) were maintained and prepared for cytotoxicity and
245 membrane potential variation assays as previously detailed [33,34]. Lyophilized crude venoms
246 were solubilized in ultra-pure water and diluted in culture medium before being exposed to cells at
247 various final concentrations (from $1 \text{ ng}/\text{mL}$ to $100 \mu\text{g}/\text{mL}$) for 24 h at 25°C for cytotoxic assays or
248 at $100 \mu\text{g}/\text{mL}$ for 30 min at 25°C for membrane potential monitoring. Cytotoxic assays were
249 performed using lysis buffer and culture medium as positive and negative controls or blanks,
250 respectively. Membrane potential changes were measured using a buffer containing: 115 mM
251 NaCl, 5 mM KCl, 2 mM CaCl_2 , 1 mM MgCl_2 , 48 mM sucrose, and 10 mM HEPES. The assays
252 and calculations of LC_{50} were performed as previously described [33].

253 **(g) Phylogenetic analysis**

254 To generate a phylogeny of the studied species we searched for conserved genes across their
255 transcriptome assemblies, or genome for *Pa. clavata*, using BUSCO v5.1.2 [35]. Using the
256 hymenoptera_odb10 database, we identified 566 genes present in at least 90% of the species.
257 We aligned the protein sequences from each gene using mafft and concatenated them into a
258 supermatrix (Dataset S2). Then, we used IQTREE2 v2.1.2 [36] to reconstruct the maximum
259 likelihood tree by using the concatenated matrix and the selection of the best substitution model
260 with ModelFinder and 1000 ultrafast bootstrap replicates. Ancestral states reconstruction for

261 venom activities and capacities, were estimated by maximum likelihood using the `contmap` ()
262 function of the `Phytools` R package with default settings [37]. To test for statistical support for
263 correlations between venom bioactivities and morphological traits, and the influences of
264 ecological traits, we used the phylogenetic Generalized Least Squares (PGLS) approach using
265 the `PGLS` () function of the "caper" package in RStudio. We examined the correlation between
266 each pair of traits individually with the formula set as ([functional traits, e.g. `vertebrate_pain`] ~
267 grouping [ecological traits, e.g. `defensive_use` (yes or no)] and `lambda` set to "Maximum
268 Likelihood". For the PGLS regressions, we treated log-transformed continuous traits.

269 3. Results and Discussion

270 (a) Ecological and venom-related traits

271 First, we collected observational data about the diet and the use of venom during prey capture or
272 defense to fill the ecological knowledge gap for the studied species. These observations enabled
273 us to define the ecological traits of all the species studied (Figure 1). We did not retain diet
274 specialization as an ecological trait for further analysis since *A. emarginatus* appeared to be an
275 euryphagous predator (i.e. prey on numerous classes of invertebrates) (electronic supplementary
276 material, figure S1) like all other predatory species included in our study, except for *N.*
277 *commutata*. Additional ecological observations are presented in Figure S13.

278 We then measured how venom-related traits varied among the 15 ant species (electronic
279 supplementary material, figures S14, S15, and S16). All the morphological data and proportions
280 related to venom yield, venom reservoir volume, sting length, and mandibles length are presented
281 in electronic supplementary material, Table S1 and Table S2. *Pseudomyrmex penetrator* and *Pa.*
282 *clavata* had the longest stings with ratios of 0.58 and 0.55 and *Odontomachus* spp., *A.*
283 *emarginatus*, and *P. gracilis* the shortest (ratios ranged from 0.32 to 0.41) (electronic
284 supplementary material, figure S14, E, and Table S1). *Pa. clavata* and *D. armigerum* were the
285 species with the longest mandibles with ratios of 1.0 and 1.1, while *P. penetrator*, *P. viduus* and
286 *P. gracilis* have short mandibles with an average ratio of 0.4 (electronic supplementary material,
287 figure. S14, F and Table S1). We also evaluated the potency of the 15 venoms to trigger
288 nociception in vertebrates and to paralyze and to kill invertebrate prey (electronic supplementary
289 material Tables S3 and S4). The capacity of the venom of a given species is a product of both the
290 venom potency and the amount of venom delivered. To be able to compare species, we therefore
291 calculated both their nocifensive capacity (pain-inducing) and paralytic capacity by dividing the
292 average venom yield (μg) by venom potency ($\mu\text{g/mL}$) (see details in electronic supplementary
293 material, Tables S3 and S4).

294 Of the 15 venoms tested with concentrations up to 100 $\mu\text{g/mL}$, 14 caused an increase in
295 $[\text{Ca}^{2+}]$ in the neuronal cell assays (electronic supplementary material, Figure S15), revealing
296 variation in the potency of the different venoms to induce pain (electronic supplementary
297 material, Table S3). The venom of *D. armigerum* was inactive, while that of *A. emarginatus* was
298 active only at the highest concentration tested (100 $\mu\text{g/mL}$). The estimated median effective
299 concentration (EC_{50}) for the venoms of *D. armigerum*, *A. emarginatus*, *P. viduus*, and *O. scalptus*
300 were estimated to be $>100 \mu\text{g/mL}$; those of *O. mayi*, *N. commutata*, *O. haematodus*, *O. hastatus*,
301 and *P. gracilis* venoms ranged from 69 (*O. mayi*) to 98 (*P. gracilis*) $\mu\text{g/mL}$; The venoms of *P.*
302 *termitarius*, *N. inversa*, *N. goeldii*, *N. apicalis*, and *P. penetrator* were more potent with EC_{50}
303 ranging from 20 (*P. penetrator*) to 53 (*P. termitarius*) $\mu\text{g/mL}$; The venom of *Pa. clavata* was the
304 most potent of those tested with an EC_{50} of 3.7 $\mu\text{g/mL}$. *Daceton armigerum*, *A. emarginatus*, and
305 *P. gracilis* have the lowest estimated nocifensive capacities of the species tested; These are
306 followed by *P. viduus*, *O. mayi*, *O. scalptus*, *P. termitarius*, *O. haematodus*, and *P. penetrator*;

307 The species *O. hastatus*, *N. goeldii*, *N. apicalis*, *N. inversa*, and *N. commutata* have estimated
308 nocifensive capacities that are an order of magnitude greater; finally, *Pa. clavata* has the greatest
309 estimated nocifensive capacity of all of tested species.

310 All of the tested venoms caused paralysis in blowflies but with different potencies
311 (electronic supplementary material, Figure S16 and Table S4). At 1 h, the venoms of *D.*
312 *armigerum*, *A. emarginatus*, *P. penetrator*, *P. viduus*, and *P. termitarius* were the most potent
313 paralytic venoms with median paralytic doses (PD₅₀) ranging from 1.2 to 12.9 µg/g, while
314 *Odontomachus* spp. venoms affected the blowflies only at high doses (PD₅₀ range from 105.6 to
315 179.2 µg/g). The venoms of *Neoponera* spp., *P. gracilis*, and *Pa. clavata* had mild paralytic
316 activity (PD₅₀ range from 47.4 to 99.6 µg/g). The paralytic effect of *Pa. clavata* venom was
317 reversible and dissipated rapidly, with all blowflies recovering 24 h post-injection except at the
318 highest dose injected (PD_{50_24h} = 265.7 ± 14.5 µg/g), whereas with all other venoms, blowflies
319 remained affected (paralyzed or dead) 24h post-injection. Mild/low lethality was observed, with
320 median lethal doses (LD₅₀) for *Pa. clavata*, *A. emarginatus*, *Neoponera* spp., *Odontomachus*
321 spp., and *P. gracilis* venoms ranging from 245.9 to 677.6 µg/g. By contrast, the venoms of *D.*
322 *armigerum*, *P. viduus*, *P. termitarius*, and *P. penetrator* were highly lethal (LD₅₀ ranged from 2.0
323 to 15.5 µg/g). The venom yields allowed us to calculate the paralyzing and lethal capacities of
324 each species. The paralytic capacities at 1 h were particularly high for *P. viduus*, *N. commutata*,
325 and *Pa. clavata* with values of 16.7, 14.6, and 4.6, respectively. These are followed by *P.*
326 *penetrator*, *D. armigerum*, *N. inversa*, *P. termitarius*, and *A. emarginatus* with values between 1
327 and 2.3. *Odontomachus* spp., *N. goeldii*, *N. apicalis*, and *P. gracilis* had low paralytic capacities
328 with values <1.

329 We then evaluated the cytotoxicity of the venoms to gain insight into their mechanism of
330 action. At a concentration of 100 µg/mL, all crude venoms except those of *A. emarginatus* and *D.*
331 *armigerum* were cytotoxic on *Drosophila* cells (electronic supplementary material, figure S17).
332 The venoms of *Odontomachus* spp. were only cytotoxic at high doses, affecting cell metabolism
333 with LC₅₀ values ranging from 15.8 to 42.9 µg/mL and cell membranes with LC₅₀ values ranging
334 from 18.5 to 49.0 µg/mL. The venoms of *Neoponera* spp. were more cytotoxic with LC₅₀ ranging
335 from 5.5 to 8.3 µg/mL and from 5.8 to 14.8 µg/mL for cell metabolism and cell membrane integrity
336 assays, respectively. The *Pseudomyrmex* spp. venoms were very cytotoxic, and the venoms of *P.*
337 *penetrator* and *P. termitarius* were the most potent, impacting both cell metabolism (LC₅₀ of 0.05
338 and 0.24 µg/mL for *P. penetrator* and *P. termitarius*) and cell membrane integrity (LC₅₀ of 0.08
339 and 0.23 µg/mL for *P. penetrator* and *P. termitarius*). *Pa. clavata* venom was cytotoxic but was
340 more potent on cell metabolism (LC₅₀ of 2.72 µg/mL) than on cell membrane integrity (LC₅₀ of
341 31.03 µg/mL). Detailed results are presented in electronic supplementary material, Table S5 and
342 Figure S17. Since no cytotoxic activity was observed for *A. emarginatus* and *D. armigerum* crude
343 venoms, to understand the mode of action we tested the neurotoxic effects of these venoms on
344 *Drosophila* cells. A significant decrease in KCl-induced membrane depolarization was observed
345 after incubation with both venoms, indicating an inhibition effect on ionic conductance (electronic
346 supplementary material, figure S18).

347 **(b) Venom-related traits reveal two functional strategies**

348 A principal component analysis (PCA) was done on the dataset including the venom activities,
349 cytotoxicity, and morphological traits. The first two axes of the PCA accounted for 76% of the total
350 variation, with axes 1 and 2 explaining 44% and 32% of the total variation, respectively (Figure
351 1A). The vertebrate pain activity and insect cell cytotoxicity have significant loading on PC1 [38]
352 while prey paralysis and sting proportion have significant loading on PC2. PCA revealed that two

353 different venom strategies are used by the studied ant species. *Anochetus emarginatus* and *D.*
354 *armigerum* can be defined as species with a non-cytotoxic venom that is capable of paralyzing
355 blowflies efficiently but has a poor capacity to induce pain in vertebrates. All other species are
356 distributed along a venom cytotoxicity gradient, with the most cytotoxic venoms causing more
357 pain in vertebrates, paralysis, and lethality in flies, and tending to have a longer sting.

358 Among ponerine species, we noted a major shift in insect paralytic activity with *A.*
359 *emarginatus*, whose venom was 13 to 22 times more paralytic than those of *Odontomachus*
360 species and at least 5 times more paralytic than those of *Neoponera* species (Figure 1B).
361 Reconstruction of the ancestral state of vertebrate pain activity illustrates how the venoms of *D.*
362 *armigerum* and *A. emarginatus* lack vertebrate pain-inducing ability (e.g. the venom of *A.*
363 *emarginatus* was 3 to 5 times less active on vertebrate sensory neurons than that of
364 *Odontomachus* species and 100 times less than that of *Pa. clavata*). The amount of venom varied
365 greatly among species, which impacts their paralytic and nocifensive capacities. It is therefore
366 worth noting that the venom of *A. emarginatus* and *D. armigerum* had a very low nocifensive
367 capacity, whereas the venom of *Pa. clavata* and to a lesser extent *N. commutata*, had a high
368 nocifensive capacity (Figure 1B). Altogether, the venom activities and capacities aligned well with
369 the ecological niche of each species. *Anochetus emarginatus* rarely stings defensively, and the
370 sting is not painful, causing only a slight itch (personal observation A.T.) which may explain the
371 cryptic lifestyle of most *Anochetus* species [39]. When disturbed, *A. emarginatus* primarily utilizes
372 its trap-jaw mandibles to bite and bounce off intruders (personal observation A.T. and [40]).
373 *Daceton armigerum* does not sting defensively (personal observation A.T.) and we showed that
374 the crude venom caused no pain-inducing activity. To avoid predation, *D. armigerum* has a very
375 thick cuticle covered with thoracic spines and has adopted an arboreal lifestyle, living in
376 polydomous nests sheltered in hollow branches [41,42]. The defensive constraint against
377 vertebrates in *Pa. clavata* and *N. commutata* may be more pronounced than in other species
378 since they ranked first and second in nocifensive capacity. The large size of workers and the fact
379 that they nest directly in the ground, makes the colony attractive in terms of nutritional resources
380 and highly vulnerable to vertebrate predation. Among ponerine ants, the venom of
381 *Odontomachus* spp. had a low paralytic activity and capacity. *Odontomachus* spp. capture their
382 prey with trap-jaw mandibles and do not always use their venom, depending on the prey type
383 [43,44]. In the *Pseudomyrmex* clade, the venom of the mutualistic plant-ant species (i.e. *P.*
384 *penetrator* and *P. viduus*) has a very high paralytic capacity on insects, in marked contrast to that
385 of *P. gracilis*. Although *P. viduus* and *P. penetrator* species do not use their venom for predation,
386 they are subject to selective pressures to defend host plants against both grazing insects and
387 vertebrates. *Pseudomyrmex penetrator* venom is also highly effective at inducing pain in
388 vertebrates (electronic supplementary material, Table S3).

389

390 (c) Correlation among traits

391 Comparative phylogenetic generalized least squares (PGLS) regression revealed several
392 significant correlations among traits (Figure 2). For the evolutionary impact of ecological traits, we
393 found that both venom use, and mandible type significantly correlate with venom bioactivities and
394 morphological traits, while there is no correlation between foraging activity (arboreal vs.
395 terrestrial-foraging species) and any other traits (Figure 2A). We show that the metabolic cost of
396 toxin secretion is reduced in stinging ant species that never use their venom for defensive
397 function, since they produce less venom than other ants (proportion of venom reservoir volume (P
398 = 0.003)). The defensive function significantly affects the properties of venom: the venoms of
399 species that use their venom defensively generally have greater cytotoxicity

400 (cytotoxicity_metabolism, $P = 0.021$; cytotoxicity_membrane, $P = 0.031$), as well as greater
401 vertebrate pain activity ($P = 0.03$), associated with higher nocifensive capacity ($P = 0.03$) than
402 species that use venom exclusively for predatory purposes (i.e. *D. armigerum*, *A. emarginatus*, *P.*
403 *gracilis*). Counterintuitively, the predatory use of venom significantly reduces the potency against
404 prey, measured as paralysis ($P = 0.024$) and lethality ($P = 0.007$) in blowflies, suggesting that
405 some predatory species may compensate low venom activity to capture prey with other
406 adaptations such as trap-jaw mandibles. Mandible strike performances vary among trap-jaw
407 species and may however have a variable influence on the venom activity [48–50]. In this study,
408 the presence of trap-jaw mandibles had no effect on venom activity against blowflies, both
409 paralysis and lethality, but was correlated with low vertebrate pain activity ($P = 0.016$), low venom
410 volume ($P = 0.022$), a smaller sting ($P = 0.010$), low nocifensive capacity ($P = 0.021$), and low
411 cytotoxicity (cytotoxicity_metabolism, $P = 0.007$; cytotoxicity_membrane, $P = 0.036$). The
412 presence of specialized mandibles was therefore associated with an overall decrease in the
413 defensive function of venom.

414 The data show that the longer the sting, the more pain activity ($P = 0.008$) and
415 cytotoxicity (cytotoxicity_metabolism, $P = 0.004$; cytotoxicity_membrane, $P = 0.002$) were found
416 in the venom, which is consistent with an anti-vertebrate role for a long sting. PLGS regression
417 showed a significant positive correlation between the venom reservoir proportion with both the
418 sting proportion and lethality in blowflies ($P = 0.011$). Pain activity in vertebrates was strongly
419 positively correlated with the cytotoxicity of venoms (cytotoxicity_metabolism, $P < 0.001$;
420 cytotoxicity_membrane, $P = 0.002$) but negatively correlated with the paralysis in blowflies
421 (blowfly_paralysis_1h, $P = 0.018$; blowfly_paralysis_24h, $P = 0.014$) (Figure 2B). This is
422 suggestive of a trade-off between vertebrate pain-inducing activity and insect-predation activity in
423 these ant venoms. Such a trade-off might translate to life history strategies, where species with
424 potent paralytic venom against prey have reduced capacity to deter vertebrate predators and are
425 therefore prone to adopt alternative defensive strategies, such as cryptic habits, nesting
426 strategies (e.g. polydomous nest) or promoting behavioral (e.g. thanatosis or escape behavior)
427 and morphological (e.g. thick cuticle and spines; body size reduction) anti-predation co-
428 adaptations.

429 **(d) The venom composition of stinging ants**

430 To understand the biochemical mechanisms underlying the observed variations in venom
431 efficacy, we examined the venom composition of each of the 15 species (Figure 3). Overall, our
432 investigations revealed that the venoms displayed heterogeneity in composition, with a
433 considerable turnover of peptide families across genera and without any correlation with the
434 ecological traits considered (Figure 3). Most of the peptide families were genus specific with only
435 family 9 (ponericin G) shared between *Odontomachus* and *Neoponera* venoms. The venoms of
436 three species *Pa. clavata*, *A. emarginatus*, and *D. armigerum* showed a very distinctive profile
437 dominated by families of neurotoxins not shared with any other venom. Our results also showed
438 that many venom peptide families were shared by species of the same genus, but the proportion
439 varied. For further details on venom composition, see electronic supplementary material, Figures
440 S1-S12 and Dataset S1.

441 Among the species that use their venom exclusively for predation, *A. emarginatus* and *D.*
442 *armigerum* were associated with a complete shift in venom bioactivities that correlated with a
443 switch to a neurotoxic venom composition. The venom of *D. armigerum* showed a unique profile,
444 as previously reported [2], and our analysis confirmed that this venom consisted of a single family
445 of peptides (dimeric MYRTX, family 61) that displayed some amino acid sequence similarity with

446 the neurotoxic U₁₁ venom peptide from *Tetramorium bicarinatum* [34] (electronic supplementary
447 material, figure S19). Given the lack of cytotoxicity but strong paralytic activity on blowflies and
448 inhibition of cell membrane potential, these data suggested that *D. armigerum* had an insect
449 neurotoxic venom. In addition, *A. emarginatus* has a non-cytotoxic venom that is much more
450 paralytic to insects than the other ponerine venoms studied. Given the dominance of family 1
451 peptides in *A. emarginatus* venom (98% of relative expression), it is likely that 2-SS CRPXs
452 (family 1) are responsible for most, if not all, of the paralytic effects upon prey. Since one of the
453 peptides from family 1 (i.e. Ae1a) has shown inhibition (at a high concentration) on the human
454 voltage-gated calcium channel (Ca_v1), it is possible that 2-SS CRPXs are neurotoxins [45].
455 Although the venoms of *D. armigerum* and *A. emarginatus* shared similar non-cytotoxic, insect
456 neurotoxic activity, the difference in composition and the fact that they were not closely related
457 suggested that they have evolved independently. By contrast, the stings of other ponerine ants
458 *Odontomachus* spp., and *Neoponera* spp. induce sharp pain [46] and showed stronger pain
459 activity in our assay. Ponericins are very prevalent in the venom composition of *Odontomachus*,
460 *Neoponera*, and several other ponerine ants [47–49] but were not present in *A. emarginatus*
461 venom. Ponericins are multifunctional cytotoxic peptides acting on the cell membranes [50], and
462 those from the venoms of *N. apicalis* and *N. commutata* are known to cause pain in mammals
463 and to paralyze insects [46]. There is compelling evidence that membrane-active venom peptides
464 contribute to the defensive role of multiple venomous arthropods against vertebrates [51–53].

465 Neurotoxic peptides are not exclusive to ants that rely on venom solely for predation. The
466 venom of *Pa. clavata* is largely dominated by poneratoxin (family 62) [18], a pain-inducing
467 neurotoxin that modulates vertebrate voltage-gated sodium (Na_v) channels while paralyzing
468 insects only at very high doses [54]. Despite amino acid sequence similarities with other ant
469 venom peptides [54], its major toxin, poneratoxin (family 62), has never been identified from other
470 ant venoms, including the species studied here. We showed that the venom of *Pa. clavata* also
471 exhibits cytotoxicity, which is likely attributed to phospholipase A₂ (PLA₂), present in this venom at
472 higher levels than in other ants. Since *Pa. clavata* also uses its venom for predation, cytotoxicity
473 may also be a means of subduing arthropod prey. Alternatively, cytotoxicity may also be a means
474 of maintaining a multifunctional defense against predators. In this way, the venom retains a
475 general repellent effect that ensures a baseline defense of the colony in a scenario where a
476 predator would acquire resistance to neurotoxins. This hypothesis is supported by a previous
477 study of the venom of the seed-harvesting ant *Pogonomyrmex*, which uses its venom primarily for
478 defense against vertebrates, and has evolved venoms dominated by vertebrate-selective
479 peptides that target Na_v channels, but still contain a peptide that is cytotoxic to vertebrate cells
480 [55].

481 Our results indicated that the four *Pseudomyrmex* species have highly cytolytic venoms
482 and different venom profiles to other ant species, with peptide families not shared with the other
483 species studied. We found that *P. gracilis* shares few similarities with the other three
484 *Pseudomyrmex* species, and that the different venom families are present in different proportions
485 among the species. Among these families, family 39 corresponded to the myrmexins (renamed
486 here the dimeric pseudomyrmeciotoxin (PSDTX)), a group of dimeric peptides first described in
487 the venom of *P. triplarinus* [56] which are highly cytotoxic to insect cells [57]. Dimeric PSDTXs
488 largely dominated the venom of *P. viduus* (94% of relative venom expression), which was found
489 to be the most paralytic and lethal venom on blowflies. The other families consisted of cysteine-
490 free polycationic peptides which may also contribute to the observed cytotoxicity by disrupting cell
491 membranes. The venom of *P. penetrator* was at least 3 times more cytotoxic than in other
492 *Pseudomyrmex*, at least 72 times more cytotoxic than *Neoponera*, and at least 231 times more

493 cytotoxic than *Odontomachus* (electronic supplementary material, Table S5). This was associated
494 with high efficacy for inducing pain in vertebrates and paralyzing insects. This example highlights
495 the fact that the trade-off between vertebrate and insect-predatory venom activity may be
496 disrupted by very high cytotoxicity.

497 **4. Conclusion**

498 Venoms are under strong evolutionary pressures, exerted either on the innovation of toxins or the
499 reduction of the metabolic cost of production. Many ants use venom for subduing a wide range of
500 arthropod prey, as well as for defensive purposes against invertebrates and vertebrates, but are
501 unable to adapt venom composition to stimuli [52,58]. Consequently, the expression of venom
502 genes directly affects the ability of ants to interact with the biotic environment, and the venom
503 composition may be fine-tuned to the ecology of each species. A previous study showed that
504 defensive traits in ants exhibit an evolutionary trade-off in which the presence of a sting is
505 negatively correlated with several other defensive traits, further supporting that trade-offs in
506 defensive traits significantly constrain trait evolution and influence species diversification in ants
507 [17]. However, the sting is not used for the same purpose depending on the ant species. In this
508 study we use a multi-pronged approach to test foraging activity, venom function, and mandible
509 morphology as evolutionary drivers underlying venom variation in ants. We show that ant venoms
510 can be highly heterogeneous and that there have been major shifts in venom composition and
511 bioactivities, even among phylogenetically closely related species. Among the ant species
512 investigated, we found that foraging activity had no impact on venom, but the ecological role of
513 the venom, offensive or defensive, and even more so the breadth of biological targets, were
514 arguably dominant constraints in the evolution of the venom cocktail of these stinging ants.
515 Metering the amount of venom produced is potentially the swiftest way to adapt to different
516 ecological constraints [59] such as for *N. commutata*, which has a quite similar venom
517 composition profile to other congeneric ponerine species but produces large amounts of venom.
518 Evolution may further fine-tune venom composition toward ecologically relevant cocktails
519 exhibiting different functional strategies based on either neurotoxins or cytotoxins. Cytotoxic
520 toxins, which do not require a specific pharmacological receptor, are likely to offer an evolutionary
521 advantage to species that need to target a wide range of both vertebrate and arthropod
522 organisms with highly divergent nervous systems. In some lineages of ants, however, evolution
523 may have favored neurotoxin-based venoms as the range of biological targets narrowed. A
524 reasonable explanation for the prevalence of neurotoxic-based venoms in ants would be that
525 cytotoxic peptides often act at high concentrations compared to neurotoxins [54], and are
526 therefore likely to be associated with higher metabolic costs. Although broader phylogenetic
527 coverage is needed to confirm these findings, our results illustrate the importance of combining
528 functional data with venom investigations to understand the drivers underlying venom evolution.

529 **Data availability.** The raw sequencing reads used in this manuscript are available from the
530 National Center for Biotechnology Information (NCBI) under the project code PRJNA1061791.
531 The mass spectrometry proteomics data have been deposited to the ProteomeXchange
532 Consortium via the PRIDE partner repository with the dataset identifier PXD050348.

533

534 **References**

535

536

- 537 1. Touchard A, Aili SR, Fox EGP, Escoubas P, Orivel J, Nicholson GM, Dejean A. 2016 The
538 Biochemical Toxin Arsenal from Ant Venoms. *Toxins* **8**. (doi:10.3390/toxins8010030)
- 539 2. Barassé V *et al.* 2022 Venomics survey of six myrmicine ants provides insights into the
540 molecular and structural diversity of their peptide toxins. *Insect Biochem. Mol. Biol.* **151**,
541 103876.
- 542 3. Touchard A, Koh JMS, Aili SR, Dejean A, Nicholson GM, Orivel J, Escoubas P. 2015 The
543 complexity and structural diversity of ant venom peptidomes is revealed by mass
544 spectrometry profiling. *Rapid Commun. Mass Spectrom.* **29**, 385–396.
- 545 4. Wilson EO, Hölldobler B. 2005 The rise of the ants: a phylogenetic and ecological
546 explanation. *Proc. Natl. Acad. Sci. U. S. A.* **102**, 7411–7414.
- 547 5. Orivel J, Dejean A. 2001 Comparative effect of the venoms of ants of the genus
548 *Pachycondyla* (Hymenoptera: Ponerinae). *Toxicon* **39**, 195–201.
- 549 6. Casewell NR, Wüster W, Vonk FJ, Harrison RA, Fry BG. 2013 Complex cocktails: the
550 evolutionary novelty of venoms. *Trends Ecol. Evol.* **28**, 219–229.
- 551 7. Cerdá X, Dejean A. 2011 Predation by ants on arthropods and other animals. *National*
552 *Academy of Sciences (US)*
- 553 8. Michálek O, Kuhn-Nentwig L, Pekár S. 2019 High Specific Efficiency of Venom of Two Prey-
554 Specialized Spiders. *Toxins* **11**. (doi:10.3390/toxins11120687)
- 555 9. Phuong MA, Mahardika GN, Alfaro ME. 2016 Dietary breadth is positively correlated with
556 venom complexity in cone snails. *BMC Genomics* **17**, 401.
- 557 10. Lyons K, Dugon MM, Healy K. 2020 Diet Breadth Mediates the Prey Specificity of Venom
558 Potency in Snakes. *Toxins* **12**. (doi:10.3390/toxins12020074)
- 559 11. Booher DB *et al.* 2021 Functional innovation promotes diversification of form in the evolution
560 of an ultrafast trap-jaw mechanism in ants. *PLoS Biol.* **19**, e3001031.
- 561 12. Larabee FJ, Suarez AV. 2014 The evolution and functional morphology of trap-jaw ants
562 (Hymenoptera: Formicidae). *Myrmecol. News* **20**, 25–36.
- 563 13. Rubin BER, Kautz S, Wray BD, Moreau CS. 2019 Dietary specialization in mutualistic
564 acacia-ants affects relative abundance but not identity of host-associated bacteria. *Mol. Ecol.*
565 **28**, 900–916.
- 566 14. Jelley C, Moreau CS. 2023 Aggressive behavior across ant lineages: importance,
567 quantification, and associations with trait evolution. *Insectes Soc.*
- 568 15. Cardoso DC, Alves ICC, Cristiano MP, Heinze J. 2024 Death feigning in ants. *Myrmecol.*
569 *News* **34**.
- 570 16. Grasso DA, Giannetti D, Castracani C, Spotti FA, Mori A. 2020 Rolling away: a novel
571 context-dependent escape behaviour discovered in ants. *Sci. Rep.* **10**, 3784.
- 572 17. Blanchard BD, Moreau CS. 2017 Defensive traits exhibit an evolutionary trade-off and drive
573 diversification in ants. *Evolution* **71**, 315–328.
- 574 18. Aili SR *et al.* 2020 An integrated proteomic and transcriptomic analysis reveals the venom
575 complexity of the bullet ant *Paraponera clavata*. *Toxins* **12**. (doi:10.3390/toxins12050324)
- 576 19. Mill AE. 1984 Predation by the ponerine ant *Pachycondyla commutata* on termites of the
577 genus *Syntermes* in Amazonian rain forest. *J. Nat. Hist.* **18**, 405–410.
- 578 20. Dejean A, Olmsted I. 1997 Ecological studies on *Aechmea bracteata* (Swartz)
579 (Bromeliaceae). *J. Nat. Hist.* **31**, 1313–1334.
- 580 21. Schatz B, Orivel J, Lachaud J-P, Beugnon G, Dejean A. 1999 Sitemate recognition: the case
581 of *Anochetus traegordhi* (Hymenoptera; Formicidae) preying on *Nasutitermes* (Isoptera:
582 Termitidae). *Sociobiology* **34**, 569–580.
- 583 22. Piek T, Duval A, Hue B, Karst H, Lapied B, Mantel P, Nakajima T, Pelhate M, Schmidt JO.
584 1991 Poneratoxin, a novel peptide neurotoxin from the venom of the ant, *Paraponera*
585 *clavata*. *Comp. Biochem. Physiol. C* **99**, 487–495.
- 586 23. Dejean A, Labrière N, Touchard A, Petitclerc F, Roux O. 2014 Nesting habits shape feeding
587 preferences and predatory behavior in an ant genus. *Naturwissenschaften* **101**, 323–330.
- 588 24. Kazandjian TD *et al.* 2021 Convergent evolution of pain-inducing defensive venom
589 components in spitting cobras. *Science* **371**, 386–390.

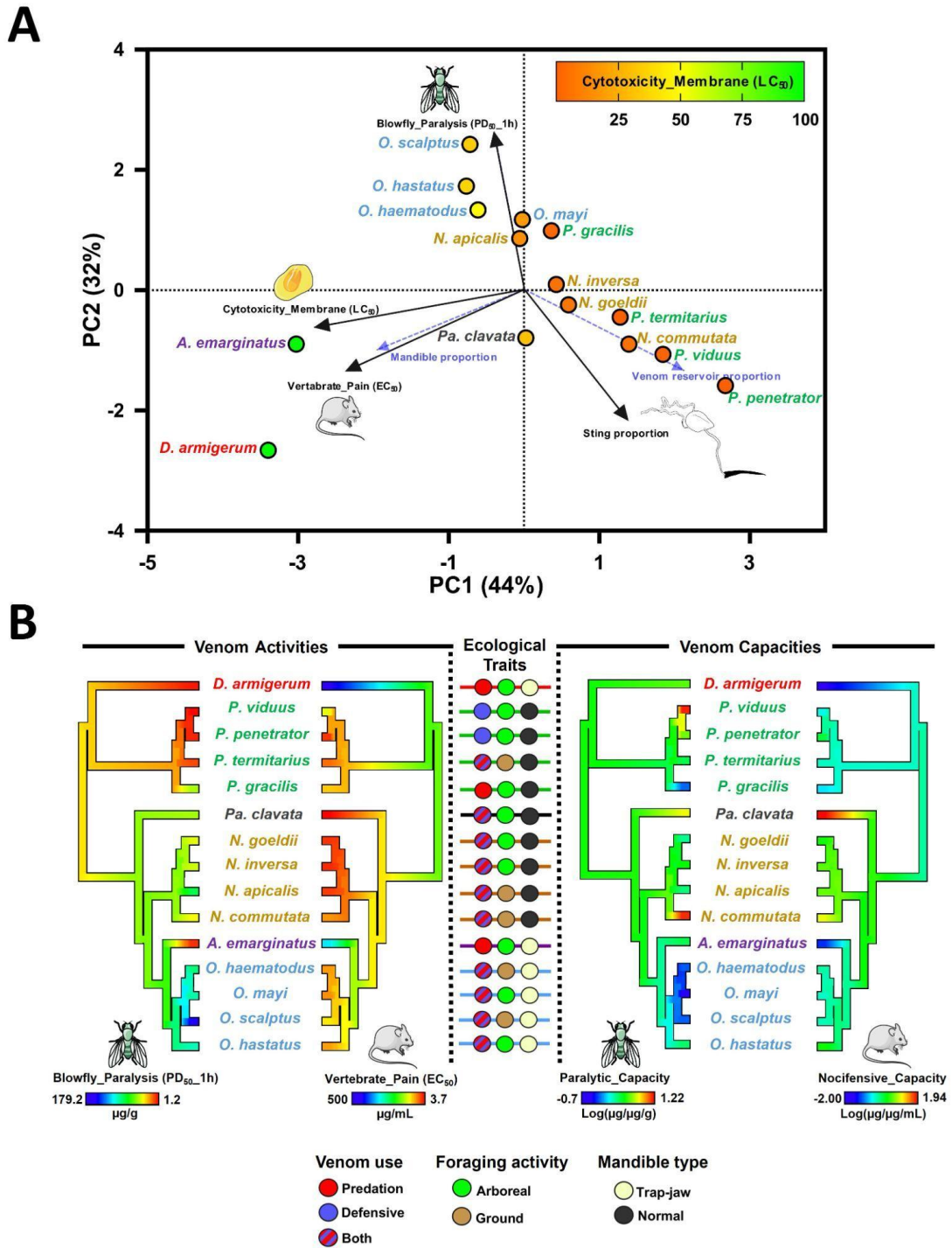
- 590 25. Zhang J *et al.* 2012 PEAKS DB: de novo sequencing assisted database search for sensitive
591 and accurate peptide identification. *Mol. Cell. Proteomics* **11**, M111.010587.
- 592 26. Teufel F *et al.* 2022 SignalP 6.0 predicts all five types of signal peptides using protein
593 language models. *Nat. Biotechnol.* **40**, 1023–1025.
- 594 27. Kumar S, Stecher G, Li M, Knyaz C, Tamura K. 2018 MEGA X: Molecular Evolutionary
595 Genetics Analysis across Computing Platforms. *Mol. Biol. Evol.* **35**, 1547–1549.
- 596 28. Waterhouse AM, Procter JB, Martin DMA, Clamp M, Barton GJ. 2009 Jalview Version 2—a
597 multiple sequence alignment editor and analysis workbench. *Bioinformatics* **25**, 1189–1191.
- 598 29. Dixon P. 2003 VEGAN, a package of R functions for community ecology. *J. Veg. Sci.* **14**,
599 927–930.
- 600 30. R Core Team R, Others. 2013 R: A language and environment for statistical computing.
- 601 31. Galili T. 2015 dendextend: an R package for visualizing, adjusting and comparing trees of
602 hierarchical clustering. *Bioinformatics* **31**, 3718–3720.
- 603 32. Weber NA. 1938 The biology of the fungus-growing ants. Part 4. Additional new forms. Part
604 5. The Attini of Bolivia. *Revista De Entomologia* **9**, 154–206.
- 605 33. Ascoët S *et al.* 2023 The mechanism underlying toxicity of a venom peptide against insects
606 reveals how ants are master at disrupting membranes. *iScience* **26**, 106157.
- 607 34. Barassé V *et al.* 2023 Discovery of an insect neuroactive helix ring peptide from ant venom.
608 *Toxins* **15**. (doi:10.3390/toxins15100600)
- 609 35. Simão FA, Waterhouse RM, Ioannidis P, Kriventseva EV, Zdobnov EM. 2015 BUSCO:
610 assessing genome assembly and annotation completeness with single-copy orthologs.
611 *Bioinformatics* **31**, 3210–3212.
- 612 36. Minh BQ, Schmidt HA, Chernomor O, Schrempf D, Woodhams MD, von Haeseler A, Lanfear
613 R. 2020 IQ-TREE 2: New Models and Efficient Methods for Phylogenetic Inference in the
614 Genomic Era. *Mol. Biol. Evol.* **37**, 2461.
- 615 37. Revell LJ. 2012 phytools: an R package for phylogenetic comparative biology (and other
616 things). *Methods Ecol. Evol.* **3**, 217–223.
- 617 38. Camargo A. 2022 PCAtest: testing the statistical significance of Principal Component
618 Analysis in R. *PeerJ* **10**, e12967.
- 619 39. Schmidt C. 2013 Molecular phylogenetics of ponerine ants (Hymenoptera: Formicidae:
620 Ponerinae). *Zootaxa* **3647**, 201–250.
- 621 40. Gibson JC, Larabee FJ, Touchard A, Orivel J, Suarez AV. 2018 Mandible strike kinematics
622 of the trap-jaw ant genus *Anochetus* Mayr (Hymenoptera: Formicidae). *J. Zool.* **306**, 119–
623 128.
- 624 41. Dejean A, Delabie JHC, Corbara B, Azémar F, Groc S, Orivel J, Leponce M. 2012 The
625 ecology and feeding habits of the arboreal trap-jawed ant *Daceton armigerum*. *PLoS One* **7**,
626 e37683.
- 627 42. Van Wilgenburg E, Elgar MA. 2007 Colony characteristics influence the risk of nest
628 predation of a polydomous ant by a monotreme. *Biol. J. Linn. Soc. Lond.* **92**, 1–8.
- 629 43. De la Mora A, Pérez-Lachaud G, Lachaud J-P. 2008 Mandible strike: the lethal weapon of
630 *Odontomachus opaciventris* against small prey. *Behav. Processes* **78**, 64–75.
- 631 44. Carlin NF, Gladstein DS. 1989 The ‘bouncer’ defense of *Odontomachus Ruginodis* and other
632 odontomachine ants (Hymenoptera: Formicidae). *Psyche* **96**, 1–19.
- 633 45. Touchard A *et al.* 2016 Isolation and characterization of a structurally unique β -hairpin
634 venom peptide from the predatory ant *Anochetus emarginatus*. *Biochim. Biophys. Acta* **1860**,
635 2553–2562.
- 636 46. Nixon SA *et al.* 2021 Multipurpose peptides: The venoms of Amazonian stinging ants contain
637 anthelmintic ponerocins with diverse predatory and defensive activities. *Biochem. Pharmacol.*
638 **192**, 114693.
- 639 47. Johnson SR, Copello JA, Evans MS, Suarez AV. 2010 A biochemical characterization of the
640 major peptides from the Venom of the giant Neotropical hunting ant *Dinoponera australis*.
641 *Toxicon* **55**, 702–710.

- 642 48. Orivel J, Redeker V, Le Caer JP, Krier F, Revol-Junelles AM, Longeon A, Chaffotte A,
643 Dejean A, Rossier J. 2001 Ponericins, new antibacterial and insecticidal peptides from the
644 venom of the ant *Pachycondyla goeldii*. *J. Biol. Chem.* **276**, 17823–17829.
- 645 49. Kazuma K, Masuko K, Konno K, Inagaki H. 2017 Combined venom gland transcriptomic and
646 venom peptidomic analysis of the predatory ant *Odontomachus monticola*. *Toxins* **9**, 323.
- 647 50. Lv S *et al.* 2022 Highly selective performance of rationally designed antimicrobial peptides
648 based on ponericin-W1. *Biomater Sci* **10**, 4848–4865.
- 649 51. Walker AA *et al.* 2021 Production, composition, and mode of action of the painful defensive
650 venom produced by a limacodid caterpillar, *Doratifera vulnerans*. *Proc. Natl. Acad. Sci. U. S.*
651 *A.* **118**. (doi:10.1073/pnas.2023815118)
- 652 52. Robinson SD, Mueller A, Clayton D, Starobova H, Hamilton BR, Payne RJ, Vetter I, King
653 GF, Undheim EAB. 2018 A comprehensive portrait of the venom of the giant red bull ant,
654 *Myrmecia gulosa*, reveals a hyperdiverse hymenopteran toxin gene family. *Sci Adv* **4**,
655 eaau4640.
- 656 53. Jensen T, Walker AA, Nguyen SH, Jin A-H, Deuis JR, Vetter I, King GF, Schmidt JO,
657 Robinson SD. 2021 Venom chemistry underlying the painful stings of velvet ants
658 (Hymenoptera: Mutillidae). *Cell. Mol. Life Sci.* **78**, 5163–5177.
- 659 54. Robinson SD *et al.* 2023 Ant venoms contain vertebrate-selective pain-causing sodium
660 channel toxins. *Nat. Commun.* **14**, 2977.
- 661 55. Robinson SD *et al.* 2024 Peptide toxins that target vertebrate voltage-gated sodium
662 channels underly the painful stings of harvester ants. *J. Biol. Chem.* **300**, 105577.
- 663 56. Pan J, Hink WF. 2000 Isolation and characterization of myrmexins, six isoforms of venom
664 proteins with anti-inflammatory activity from the tropical ant, *Pseudomyrmex triplarinus*.
665 *Toxicon* **38**, 1403–1413.
- 666 57. Touchard A *et al.* 2020 Heterodimeric Insecticidal Peptide Provides New Insights into the
667 Molecular and Functional Diversity of Ant Venoms. *ACS Pharmacol Transl Sci* **3**, 1211–
668 1224.
- 669 58. Schendel V, Rash LD, Jenner RA, Undheim EAB. 2019 The diversity of venom: The
670 importance of behavior and venom system morphology in understanding its ecology and
671 evolution. *Toxins* **11**. (doi:10.3390/toxins11110666)
- 672 59. Koenig PA, Moreau CS. 2023 Testing optimal defence theory in a social insect: Increased
673 risk is correlated with increased venom investment. *Ecol. Entomol.* (doi:10.1111/een.13295)

674

675

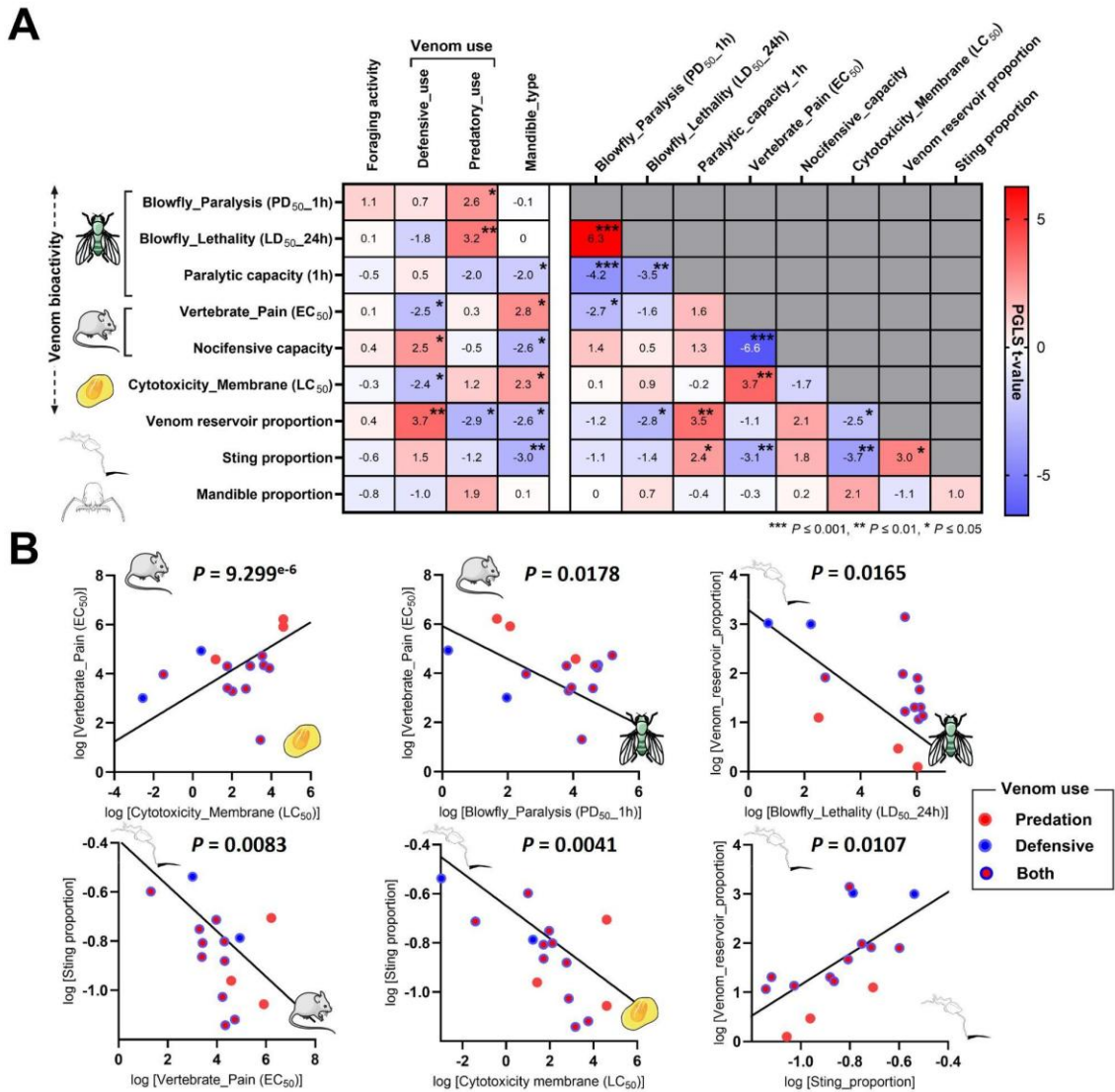
676 **Figures**



677

678 **Figure 1.** Venom bioactivity and morphological traits in 15 ant species. A) Principal component
 679 analysis of 15 ant species defined by venom bioactivities and morphological features. PCA
 680 revealed two functional strategies among species based on the cytotoxicity of venom. The
 681 significance of each PC axis, and of loading of each trait have been tested by the PCAtest R
 682 package [66]. Traits having significant loadings on PC 1 and PC 2 are represented with black
 683 arrows, while others are represented with dashed blue arrows. Plot points are colored in a

684 gradient based on membrane cytotoxicity values (LD_{50}) as indicated by the scale bar at the top
685 right. See also electronic supplementary materials, figure S7 for PCA on the dataset featuring all
686 traits. B) Ancestral state reconstructions of the insect paralytic activity (PD_{50_1h}), vertebrate pain
687 activity (EC_{50}), paralytic capacity, and nocifensive capacity of crude ant venoms, estimated by
688 using the Phytools R package [67]. Since *D. armigerum* venom was inactive on F11 cells, we
689 used an arbitrary high value of 500 $\mu\text{g/mL}$ for vertebrate pain (EC_{50}). Capacities were calculated
690 by dividing the average venom yield (μg) by the venom potency to paralyze blowfly (PD_{50_1h} ,
691 $\mu\text{g/g}$) and to cause pain (EC_{50} , $\mu\text{g/mL}$). Venom capacities have been log-transformed. The scale
692 bar indicates trait values from low (cool colors) to high potencies (warm colors) for venom
693 activities and from low (cool colors) to high venom capacities (warm colors). The phylogenetic
694 tree was reconstructed by using transcript sequences of 566 BUSCO genes generated in this
695 study expressed in the body of ant species. Note that the results of the ancestral state
696 reconstruction could be affected by some missing ant lineages in the phylogeny. Species names
697 are colored according to genus (red for *Daceton*, purple for *Anochetus*, blue for *Odontomachus*,
698 brown for *Neoponera*, green for *Pseudomyrmex* and black for *Paraponera*).

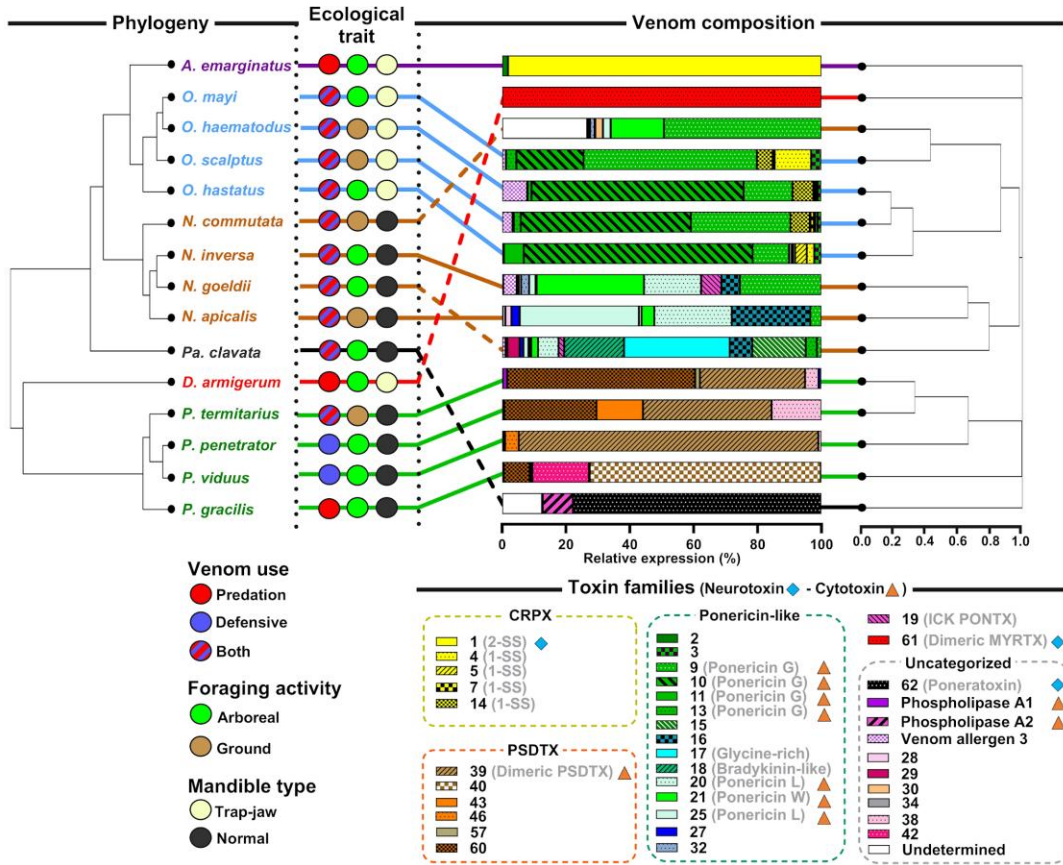


699

700 **Figure 2.** Comparative phylogenetic analysis of correlation between traits. A) Phylogenetic
 701 generalized least squares (PGLS) analysis among ecological traits, venom bioactivity, and
 702 morphological traits in the 15 ant species. As “venom use” is a multi-state discrete variable with
 703 non-ordinal properties that contain a category “both”, we decomposed that trait into two binary
 704 discrete variables (defensive_use and predatory_use) having only two states (yes or no).
 705 Heatmap with PGLS t-values and statistical significance. Positively correlated values are in red
 706 and negatively correlated values are in blue. B) PGLS linear regressions of several significantly
 707 correlated traits.

708

709



710
 711 **Figure 3.** Comparison of venom composition and phylogenetic relationships among 15 ant
 712 species. Venom composition cladogram is based on the relative expression (TMM) of transcripts
 713 identified as toxins in each venom gland transcriptome and converted into Bray-Curtis distance
 714 matrix and hierarchical cluster analysis was performed by using the complete linkage method of
 715 hclust() function with the R software. Only families with a relative expression value >1% in at
 716 least one species are shown in the color key. Toxin families are grouped by precursor clades
 717 (electronic supplementary material, figure S19). Blue diamonds and orange triangles indicate
 718 neurotoxic and cytotoxic peptide families, respectively, based on the literature. In contrast to the
 719 other species, *A. emarginatus*, *D. armigerum*, and *Pa. clavata* have convergently evolved a
 720 venom composition dominated by neurotoxic peptides.